Sedimentary Geology 282 (2012) 78–89

Contents lists available at SciVerse ScienceDirect

Sedimentary Geology

journal homepage: www.elsevier.com/locate/sedgeo

Sedimentary and foraminiferal evidence of the 2011 Tōhoku-oki tsunami on the Sendai coastal plain, Japan

Jessica E. Pilarczyk [a,b,*], Benjamin P. Horton [a], Robert C. Witter [c], Christopher H. Vane [d], Catherine Chagué-Goff [b,e], James Goff [b]

[a] Sea Level Research, Department of Earth and Environmental Science, University of Pennsylvania, 240 S. 33rd Street, Philadelphia, PA 19104-6316, USA
[b] Australia-Pacific Tsunami Research Centre, School of Biological, Earth and Environmental Sciences, University of New South Wales, Sydney 2052, Australia
[c] United States Geological Survey/Alaska Science Center, Anchorage, AK 99508, USA
[d] British Geological Survey, Keyworth, Nottingham NG92BY, UK
[e] Australian Nuclear Science and Technology Organisation, Locked Bag 2001, Kirrawee DC, NSW 2232, Australia

ARTICLE INFO

Article history:
Received 16 March 2012
Received in revised form 23 August 2012
Accepted 27 August 2012
Available online 7 September 2012

Keywords:
Sendai Plain
2011 Tohoku-oki tsunami
Jogan tsunami
Foraminifera

ABSTRACT

The 2011 Tōhoku-oki megathrust earthquake (Mw 9.0) generated a tsunami that reached the Sendai coastal plain with flow heights of ~2 to 11 m above TP (Tokyo Peil). We examined the tsunami deposit exposed in 14 shallow trenches along a ~4.5-km transect perpendicular to the coast. We primarily document the stratigraphical, sedimentological, foraminiferal and geochemical characteristics of the Tōhoku-oki tsunami deposit and perform a preliminary comparison with sediments deposited by the Jōgan tsunami of A.D. 869.

In the coastal forest and rice fields inundated by the Tōhoku-oki tsunami, a poorly sorted, dark brown soil is buried by a poorly sorted, brown, medium-grained sand deposit. In some trenches located more than 1.2 km inland, the sand is capped by a thin muddy-sand layer. The tsunami deposit, although highly variable in thickness, is generally thickest (25 cm) near the coastal dune and thins to less than 5 mm at ~4.5 km inland. The tsunami deposit was discriminated from the underlying soil by the appearance of recent and fossil foraminifera and a pronounced increase in grain size that fined upward and landward. The recent foraminifera preserved in the sandy facies of the deposit are rare and showed evidence of prolonged subaerial exposure (e.g. pitting, corrosion, fragmentation). Recent foraminifera likely originated from coastal dune and beach sediments that were breached by the tsunami. Calcified and sediment in-filled, fossil foraminifera are abundant and were eroded from sedimentary units and transported by fluvial or wave activity to Sendai Bay. Trends associated with test size (e.g. decreasing concentration of large test sizes with distance inland) are in agreement with grain size data. At two locations a decrease in total organic carbon and an increase in $\delta^{13}C$ were found in the tsunami sand compared with the underlying soil, supporting a beach to intertidal origin for the upper unit.

© 2012 Elsevier B.V. All rights reserved.

1. Introduction

Records of past tsunamis developed from the sedimentary evidence they leave behind, improve our understanding of the frequency of tsunamis by expanding the age range of events available for study (Morton et al., 2007). Proper hazard assessment depends on an awareness of tsunamis and their impacts on coastal geomorphology, ecology and rapidly expanding coastal populations. Stratigraphical sequences of tsunami deposits are often used to estimate recurrence intervals and provide insight into their source (e.g. earthquakes, landslides, volcanic eruptions; Bernard and Robinson, 2009). Reconstructions have shown repeated tsunamis during the Holocene in the Pacific northwest (Kelsey et al., 2005), North Sea (Bondevik et al., 2005), New Zealand (Goff et al., 2001), Kamchatka (Pinegina et al., 2003) and the South Pacific (Goff et al., 2011), and in the regions affected by the 1960 Chile (Cisternas et al., 2005) and 2004 Indian Ocean (e.g. Jankaew et al., 2008) earthquakes.

The identification of tsunami deposits is often based on the recognition of anomalous sand units in low-energy environments such as coastal ponds, lakes, and marshes, which can be supported by microfossil evidence. For example, the A.D. 1700 Cascadia tsunami can be identified with confidence from a sand unit that tapers landward (often for several kilometers), contains a mixed microfossil assemblage and coincides with stratigraphical evidence for abrupt coseimic subsidence (e.g. Hemphill-Haley, 1995; Hawkes et al., 2011). Foraminiferal taxonomy has been commonly used as an indicator of tsunami deposits (e.g. Mamo et al., 2009) and most taphonomic studies of foraminifera focus on time-averaging or lateral transport of tests with only semi-quantitative observations on test condition (e.g. Hawkes et al., 2007;

* Corresponding author at: Sea Level Research, Department of Earth and Environmental Science, University of Pennsylvania, 240 S. 33rd Street, Philadelphia, PA 19104-6316, USA. Tel.: +1 215 573 5145.
E-mail address: jpilar@sas.upenn.edu (J.E. Pilarczyk).

0037-0738/$ – see front matter © 2012 Elsevier B.V. All rights reserved.
http://dx.doi.org/10.1016/j.sedgeo.2012.08.011

Kortekaas and Dawson, 2007; Uchida et al., 2010). Recent research has shown that test condition provides further information regarding energy regimes and transport history (e.g. Hawkes et al., 2007; Kortekaas and Dawson, 2007; Uchida et al., 2010; Pilarczyk et al., 2011; Pilarczyk and Reinhardt, 2012a, 2012b).

The proxy toolkit to examine paleo-tsunamis has expanded following the modern surveys on the 2004 Indian Ocean and 2009 South Pacific tsunamis (Chagué-Goff et al., 2011). While geochemistry has been used for more than two decades to provide evidence for marine inundation in paleo-tsunami studies (e.g. Minoura and Nakaya, 1991; Minoura et al., 1994; Goff and Chagué-Goff, 1999; Chagué-Goff et al., 2002; Chagué-Goff, 2010), it has also recently been used in studies of modern tsunamis (e.g. Chagué-Goff et al., 2011; Chagué-Goff et al., 2012–this issue). In this study we describe foraminiferal assemblages (taxa and taphonomic), general sedimentology (grain size) and geochemistry (TOC and $\delta^{13}C$) as indicators of the 11th March 2011 Tōhoku-oki tsunami deposit. Foraminifera and sedimentological data from a trench containing the A.D. 869 Jōgan tsunami deposit are also presented. Readers are referred to Szczuciński et al. (2012–this volume) for a detailed analysis of the sedimentological and microfossil variability within the Tōhoku-oki tsunami deposit along the transect.

1.1. 2011 Tōhoku-oki tsunami

On 11th March 2011 a great megathrust earthquake (Mw 9.0) along the Japan Trench generated a tsunami that reached the Sendai plain on the northeastern coast of Honshu, Japan (Fig. 1a) at 14:46 (Japan Standard Time) with run-up heights of 10–40 m (Mori et al., 2011). The earthquake ruptured over a distance of ~400 km with upwards of 5-m vertical and 24 to 60-m lateral displacement of the seafloor (Ito et al., 2011; Sato et al., 2011). The low-lying configuration of the coastal plain made Sendai particularly susceptible to tsunami inundation that reached 4.8 km inland (Association of Japanese Geographers, 2011; Chagué-Goff et al., 2012–this issue), and sustained flooding several months after the event was documented at several locations (Sugawara et al., 2011a; Chagué-Goff et al., 2012–this issue).

1.2. A.D. 869 Jōgan tsunami

Predecessors of the Tōhoku-oki tsunami (e.g. A.D. 1611 Keichō, A.D. 1793 Kansei, A.D. 1896 Meiji Sanriku, A.D. 1933 Showa Sanriku, A.D. 1978) are numerous (Minoura and Nakaya, 1991; Minoura et al., 2001; Sawai et al., 2008a, 2008b). However, only the Jōgan tsunami in A.D. 869 is considered to approach the 2011 tsunami in terms of its magnitude, area of coastline impacted (Sendai and Sōma regions) and extent of inundation (greater than 2 km inland). On 13th July A.D. 869 an offshore earthquake approximately 200 km from the Sendai coastal plain (Fig. 1a) resulted in a large tsunami that caused widespread flooding. Estimates of the magnitude of the earthquake that generated the Jōgan tsunami, as well as flow depths and inundation distances have been investigated in an attempt to improve tsunami hazard assessments (e.g. Satake et al., 2008; Sugawara et al., 2011b).

The Jōgan deposit is a landward-thinning sand unit of variable thickness (~2–20 cm) that extends over the Sendai and Sōma regions (Sawai et al., 2008a; Sugawara and Imamura, 2010). The deposit consists of well-sorted medium sand intercalated with terrestrial organic-rich mud (Minoura et al., 2001). Overlying the Jōgan deposit is a thin soil unit that is capped by the yellowish felsic Towada-a tephra emplaced by a volcanic eruption ~250 km north of Sendai in A.D. 870–934 (Yamada and Shoji, 1981; Minoura et al., 2001; Machida and Arai, 2003). Marine and brackish water diatoms have been documented within the deposit (Minoura et al., 2001), although marine diatoms were rare in the Sendai area. Foraminifera, however, have not been studied. The tsunami sand deposit extended 2.8 km inland, however, since the Sendai plain coastline has prograded 1 km over the last ~1000 years, the inland extent of the Jōgan sand deposit is now ~4 km inland (Sawai et al., 2008b; Sugawara et al., 2011b).

2. Regional setting

The Sendai plain is a low-lying (less than 5 m above TP; Tokyo Peil; mean sea level in Tokyo Bay), wave-dominated, microtidal (mean tidal range of ~1 m) coastal plain, which extends approximately 50 km on the Pacific coast of north-eastern Japan (Fig. 1a). The area is bounded by hills to the north, west and south, and a steep continental shelf gradient (Tamura and Masuda, 2004, 2005). Early Miocene to Holocene marine and non-marine sediments dominate the coastal plain with Middle Jurassic to Early Cretaceous marine sedimentary rock outcropping to the north at Oshika Peninsula, as well as to the south near Sōma (Fig. 1b; Geological Survey of Japan, 2009). The area is characterized by a series of prograding Late Holocene beach ridges and freshwater back marshes. Sugawara et al. (2012) describe several artificial geomorphic features (e.g. breakwaters, coastal forest, Teizan canal, irrigation channels, etc.) that likely affected the run-up associated with the Tōhoku-oki tsunami but were not in place in Jōgan time. Freshwater marshes along the Sendai plain support rice cultivation, with many fields interspersed with low-density housing (Fig. 1c). Main sediment sources to the area include three rivers (the Abukuma, Natori and Nanakita rivers) that account for much of the continued seaward progradation of the coastline since the Middle Holocene (Saito, 1991; Tamura and Masuda, 2005).

The study area (near Sendai airport) consists of four key environments: coastal; coastal forest; paved landscape; and rice fields. The coastal zone transitions from intertidal marine (0.8 m below TP) to beach (1.7 m above TP) to artificial dune (2.3 m above TP; Figs. 1c, 2, and 3a) within a distance of ~0.50 km from the shoreline. The artificial dune is composed of allochthonous sediment that was brought in to armor the coastline (Fig. 2a). We do not know the origin of the dune sediment, but note that it consists of a core of loose gray sand overlain by a ~0.3-m layer of compacted, yellow-brown sand with a silt/clay matrix. We speculate that the upper compacted layer may be dredged material from nearby canals. The coastal forest (Figs. 1c and 2b), ~0.26 km from the coastline at an elevation of ~2.3 m above TP, consists of mature pine trees that were planted 300 years ago as a means of protecting rice fields from salt spray (Sugawara and Imamura, 2010). Immediately landward of the coastal forest is a paved landscape that contains several canals and a former wetland that was used for greenhouse horticulture and farming (0.10–1.20 km from coastline, ~1.0 m above TP), and rice fields (1.20–4.50 km from coastline, −0.4–1.2 m above TP).

3. Methods

3.1. Sample collection of the Tōhoku-oki tsunami deposit and geomorphology of the survey sites

In May 2011 we examined 14 trenches (Figs. 1c and 3a) containing the Tōhoku-oki tsunami deposit and its underlying soil along a transect from the coastal forest (trenches 5–9; 0.26–0.44 km inland), paved landscape (trenches 12–24; 0.54–1.23 km inland) and rice fields (trenches 31–86; 1.62–4.50 km inland). A topographic survey using a Real Time Kinematic GPS (RTK-GPS) with elevations tied to the Tokyo Peil was conducted at each sample location (Goto et al., 2011).

Trenches were sampled for sediment (0.2- to 10-cm resolution) and described in terms of deposit thickness and sedimentological composition. We examined each of the 14 trenches for lateral changes (average of all samples obtained in the tsunami deposit) associated with increasing distance inland and selected six sections for

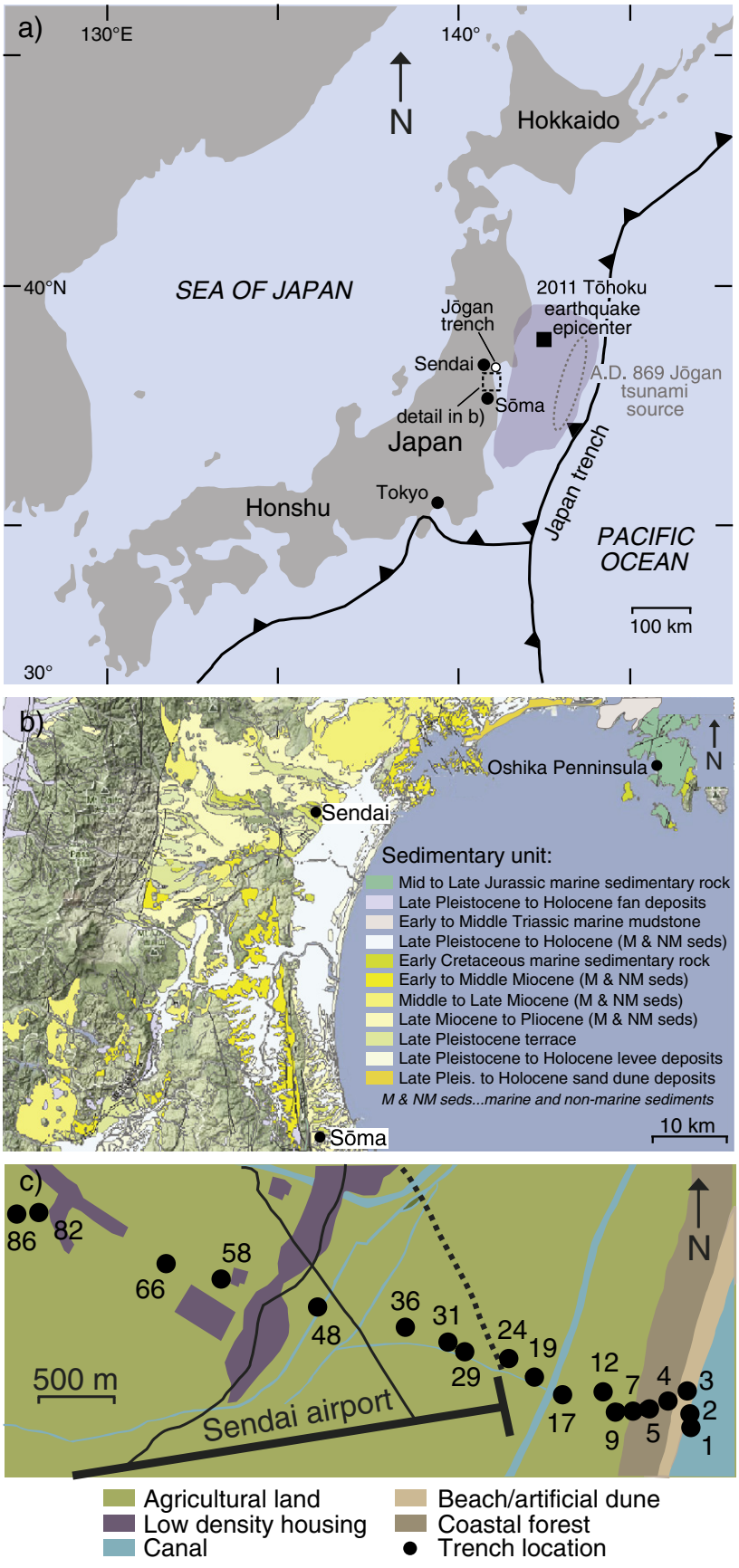

Fig. 1. (a) Map of Sendai, Japan showing broad-scale tectonics. The inferred fault zone rupture segmentation (purple shaded area) and the epicenter (black square) of the Tōhoku-oki earthquake are indicated (after Koper et al., 2011) along with the estimated source region of the A.D. 869 Jōgan tsunami (gray dotted ellipse; after Minoura et al., 2001). Location of trench transect (inset) and Jōgan trench (white circle) are indicated. (b) Geologic map of the Sendai plain and surrounding areas showing broad-scale sedimentary units (adapted from: Geological Survey of Japan, 2009). (c) Detailed map of the study area showing site locations of Tōhoku-oki trenches and surface samples (sites 1–4).

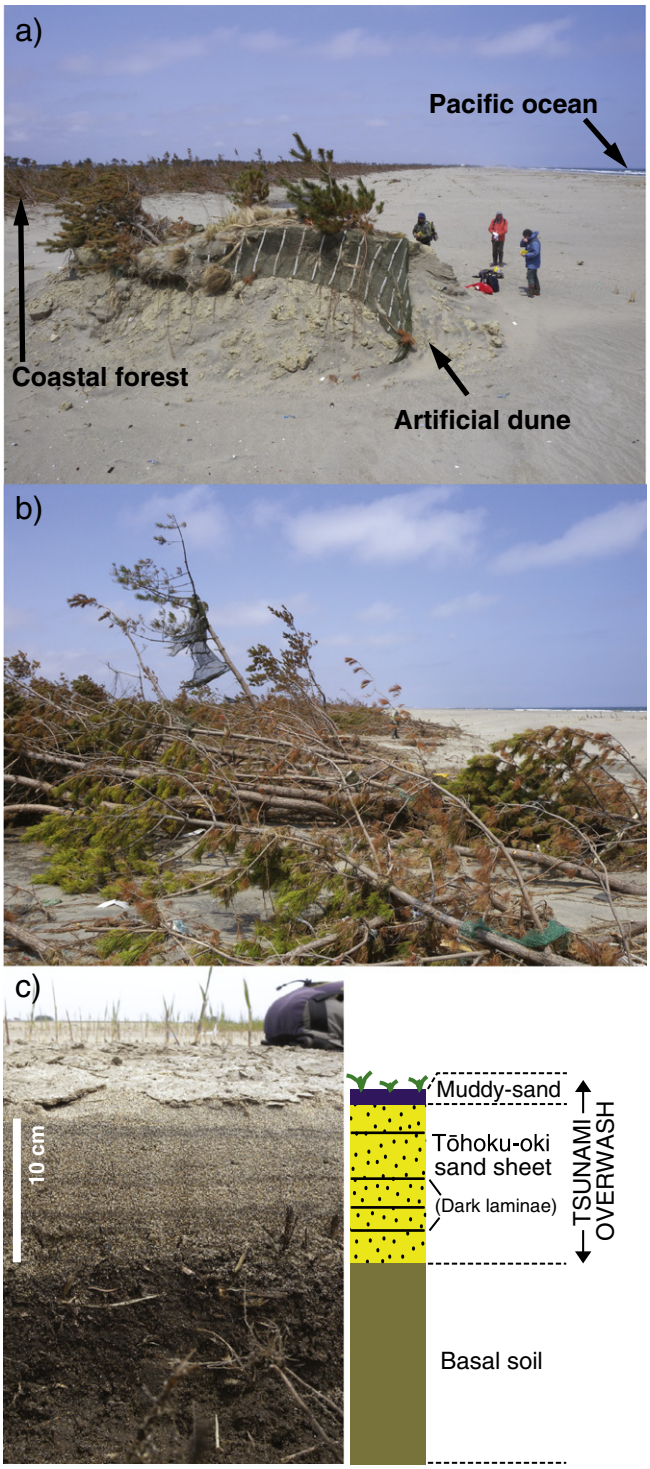

Fig. 2. (a) Remnants of the artificial dune after the Tōhoku-oki tsunami. The tsunami breached the dune in several locations and flattened pine trees and coastal shrubs, exposing an underlying stabilizing net. (b) Tsunami-flattened coastal forest planted ~300 years ago to shelter rice fields from wind and salt spray. Large pine trees were flattened in a shore-normal direction, and in some cases uprooted, as a result of the tsunami. (c) Tōhoku-oki deposit at Trench 31 (see Fig. 1c) indicating a ~10-cm-thick sand unit with a muddy-sand overlying basal rice field soil.

detailed analysis of vertical changes of the tsunami deposit with depth (e.g. trenches 5, 12, 31, 36, 48, 86). We used a node near the shoreline (38°8′27.64″N, 140°56′43.99″E) to calculate the distance of each surface sample and trench location relative to the marine source. In addition we collected surface samples (upper 1 cm) spanning the entire coastal zone (sites 1–4; −0.09 to 0.14 km inland) for comparison with tsunami sediments.

3.2. Grain size analysis

We conducted grain size analysis using a Beckman Coulter laser diffraction particle size analyzer on all bulk (e.g. no grain size fraction removed) surface and trench samples. Prior to analysis, organics were removed and samples were stirred as a moist paste to homogenize the sediment and disaggregated with sodium hexametaphosphate following the methods of Donato et al. (2009). Grain size values for all surface samples and 14 trench sections were converted to the Wentworth-Phi Scale, interpolated and gridded using a Triangular Irregular Network (TIN) algorithm according to Sambridge et al. (1995), and plotted as Particle Size Distributions (PSDs) in Geosoft Oasis TM. Grain size descriptions follow that of Blott and Pye (2001). Dominant grain size values for the 10th (D_{10}) and 90th (D_{90}) percentiles were calculated. Reporting a range of D values takes into account the skewness of a sediment distribution curve (e.g. fine tail) and can be a more suitable descriptor of grain size in non-Gaussian distributions (Blott and Pye, 2001). We used a Camsizer to calculate particle sphericity ranging from 0 (highly angular) to 1 (perfectly spherical). All grain size results are listed in Appendix 1.

3.3. Foraminiferal analysis

We conducted foraminiferal analysis on all surface and trench samples following the methods of Horton and Edwards (2006) where approximately 5-cm^3 samples were sieved (>63 μm) and examined in a liquid medium. Taxonomy followed Loeblich and Tappan (1987) and Hayward et al. (2004), and where possible, we counted up to 300 specimens (Patterson and Fishbein, 1989). Since we found no agglutinated species, samples were then dried at 25 °C, sieved and recorded as having small (<250 μm) or large (>250 μm) test sizes. We categorized individual specimens as recent (white; late Holocene) or fossil (robust, sediment in-filled and calcified; Miocene–Pleistocene; after Pilarczyk et al., 2011; Plate 1). Fossil foraminifera are easily identified since they generally maintain their test structure even after wave agitation disaggregates them from their parent rock (Pilarczyk et al., 2011). However, a long residence time in the nearshore environment results in significant abrasion and obscuring of diagnostic test features (e.g. aperture, perforations, umbo, etc.) required for proper species identification. Total number of individuals (fossil and recent individuals combined), total recent, total fossil and percent large specimens were enumerated. All foraminiferal results are listed in Appendices 2 and 3.

3.4. Stable carbon isotope and carbon analysis

For measurement of $\delta^{13}C$ and total organic carbon (TOC) in trenches, we selected two trenches (5 and 31), which include the soil, overlying sand and muddy-sand. Sediment samples were treated with 5% HCl for 18 h, washed with deionised water, dried in an oven at 40 °C overnight and milled to a fine powder using a pestle and mortar. Plant samples were treated with 5% HCl for 2–3 h, washed with deionised water, dried in an oven at 40 °C overnight and milled to a fine powder using a freezer mill (Vane et al., 2010). $^{13}C/^{12}C$ analyses were performed on sediment samples by combustion in a Costech Elemental Analyser coupled on-line to an Optima dual-inlet mass spectrometer. $\delta^{13}C$ values were calculated to the VPDB scale using a within-run laboratory standard (cellulose, Sigma Chemical prod. no. C-6413) calibrated against NBS-19 and NBS-22. Organic carbon values (TOC wt/wt) were analyzed on the same instrument. Replicate analysis indicated a precision of <0.1‰ (1 StD) for $\delta^{13}C$ and 0.1% TOC (wt/wt) measurements. All sediments reported for geochemistry were sampled over a 1-cm increment and are plotted as an average depth. With the exception of the pine roots which have

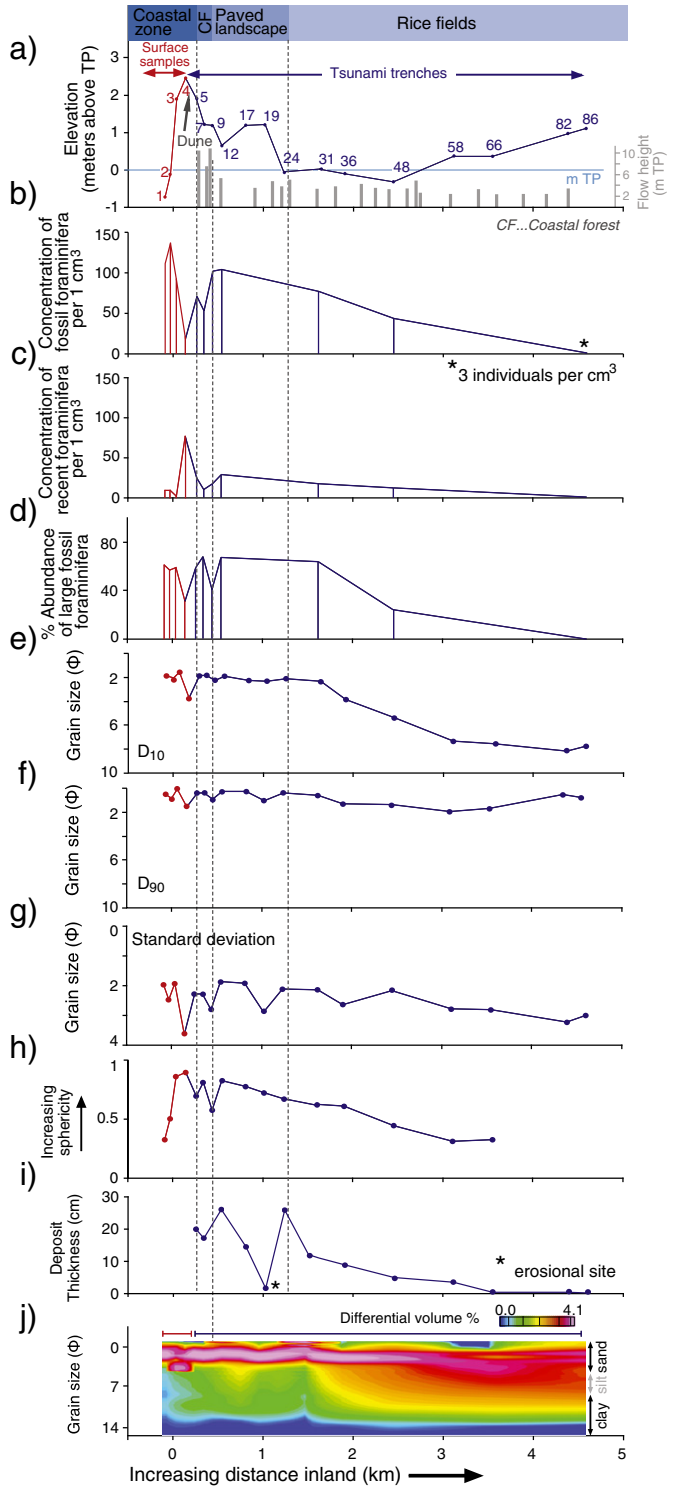

Fig. 3. Surface samples (red) compared to changes in the Tōhoku-oki deposit (blue) with increasing distance inland. (a) Elevation along a transect from the intertidal coastline of the Pacific ocean through the coastal forest, paved landscape and rice fields using the Tokyo Peil datum (TP; mean sea level in Tokyo Bay; see Fig. 1a, c). Measured tsunami flow heights are indicated in gray. (b–d) Total concentration and relative abundances of foraminiferal taphonomic data. (e–h) Average D_{10} (e), D_{90} (f), standard deviation (sorting; g), and degree of angularity (sphericity; h) data for all Tōhoku-oki deposit intervals in a single trench. Due to the dominant silt component of the deposit at trenches 82 and 86, sphericity could not be assessed. (i) Tsunami deposit thickness. Trench 19 was recovered from an area where the tsunami deposited little to no sediment but washed away existing playground equipment. (j) Average particle size distribution (PSD) plot of all tsunami deposit intervals in a single trench.

a %N of 0.6 and C/N of 85.3, the %N values were below the limit of detection (LOD) of ~0.1%, therefore C/N values were unavailable to distinguish local from imported organic matter. All $\delta^{13}C$ and TOC results are listed in Appendix 4.

3.5. Analysis of the A.D. 869 Jōgan tsunami deposit

While the Jōgan deposit has previously been documented (Minoura et al., 2001; Sawai et al., 2008a; Goto et al., 2011), we took the opportunity to log and sample a single trench containing evidence of the A.D. 869 Jōgan tsunami in a rice field ~10 km north of the Tōhoku-oki transect (Fig. 1a; 38°13′56.96″N, 140°58′33.82″E) and ~1.5 km from the present coastline. We also conducted foraminiferal and grain size analysis as outlined in Sections 3.2 and 3.3 and their results can be found in Appendices 1 and 3.

4. Results

We conducted a field survey to the north of Sendai airport (Fig. 1a) and found evidence of flow heights of 10 to 11 m above TP behind artificially emplaced dunes (Figs. 2 and 3a). Approximately 2 km from the shoreline, flow heights were noted to be 3–4 m above TP, and ~2 m above TP at a distance of 4 km from the shoreline (Goto et al., 2011). The hardest hit area was at a distance of 0–2.5 km from the shoreline where houses and roads were severely damaged and rice fields flooded with saltwater. Co-seismic subsidence (17–21 cm) approximately 10 km south of the Sendai airport was reported (Ozawa et al., 2011) as well as earthquake-induced liquefaction in the adjacent rice fields (Goto et al., 2011).

The tsunami deposited a discontinuous unit that transitioned from sand-dominated (0–2.8 km) to mud-influenced (2.8–4.5 km) sediments with increasing distance inland; Goto et al., 2011; Fig. 3). Erosion was extreme where the tsunami breached an artificially emplaced and reinforced dune system on the beach while the deposit was thickest in the coastal forest. Field descriptions of the tsunami deposit document a landward thinning and texturally fining sand to mud deposit (Appendix 1). In some trenches, the sand deposit was laminated with alternating sand and heavy mineral laminae (e.g. trench 31; Fig. 2c). Small mollusk fragments were present in very minor amounts (<1%) in intertidal and beach samples. They were also reported in the tsunami deposit but only rarely (0.2 and 0.8 km inland) and in minute amounts (<1%); Chagué-Goff et al., 2012–this issue). Richmond et al. (2012–this volume) observed articulated bivalve shells west of Teizan-bori canal and concluded that they were probably derived from the canal, as none were found on the seaward side.

4.1. Surface sediments

Grain size results distinguished between intertidal and beach samples (sites 1, 2, 3), and dune (site 4) surface samples (Fig. 3). We found coastal sediments (sites 1–4) to have similar grain sizes (D_{90} = 0.0–1.4Φ), but varying degrees of sorting (StD = 1.9–3.6Φ) and sphericity (0.3–0.9, with 1.0 being a perfect sphere). Intertidal sediment (average D_{90} = 0.5Φ), with the lowest sphericity values (0.4), was most angular in composition, followed by beach (D_{90} = 0.0Φ; sphericity = 0.8) and artificial dune sediments (D_{90} = 1.4Φ; sphericity = 0.9), which were significantly more rounded.

Surface sediment samples also showed distinctly different foraminiferal characteristics related to increasing distance away from the marine source. Intertidal samples (sites 1 and 2) had the lowest concentration of recent individuals per cm^3 (9 per cm^3), the highest concentration of fossils (124 per cm^3) and the greatest abundance of large fossil specimens (59 per cm^3). The artificial dune (site 4) was characterized by the lowest concentration of fossils (19 individuals per cm^3), but the highest concentration of recent foraminifera (77

individuals per cm^3), which were comparatively small in size (only 32% of fossils were > 250 μm). Beach sediment (site 3) marked a transition zone and had intermediate concentrations (fossil concentration = 90 individuals per cm^3; recent concentration = 2 individuals per cm^3; % large fossils = 59%). Intertidal and beach samples were predominantly composed of low abundances of miliolids (~4/cm^3; e.g. *Quinqueloculina* spp., *Triloculina* spp; Plate 1 specimens 7–10) and *Ammonia parkinsoniana* (2/cm^3), while the dune contained only marginally higher abundances (*A. parkinsoniana* = 20/cm^3, *Quinequloculina* spp. = 6/cm^3, miliolids = 51/cm^3).

4.2. Lateral changes within the Tōhoku-oki tsunami deposit

The tsunami deposit showed trends with increasing distance inland (Fig. 3b–j). In general, sediments become finer grained (average D_{10} = 1.8Φ at 0.3 km; 7.3Φ at 3.0 km; 8.1Φ at 4.5 km), less sorted (average StD = 2.3Φ at 0.3 km; 2.2Φ at 3.0 km; 2.9Φ at 4.5 km) and more angular (0.7 at 0.3 km; 0.3 at 3.0 km; 0.4 at 3.7 km) with increasing distance inland. These results are slightly coarser than those reported by Szczuciński et al. (2012–this volume) and can be attributed to differences in sampling resolution. Medium to coarse

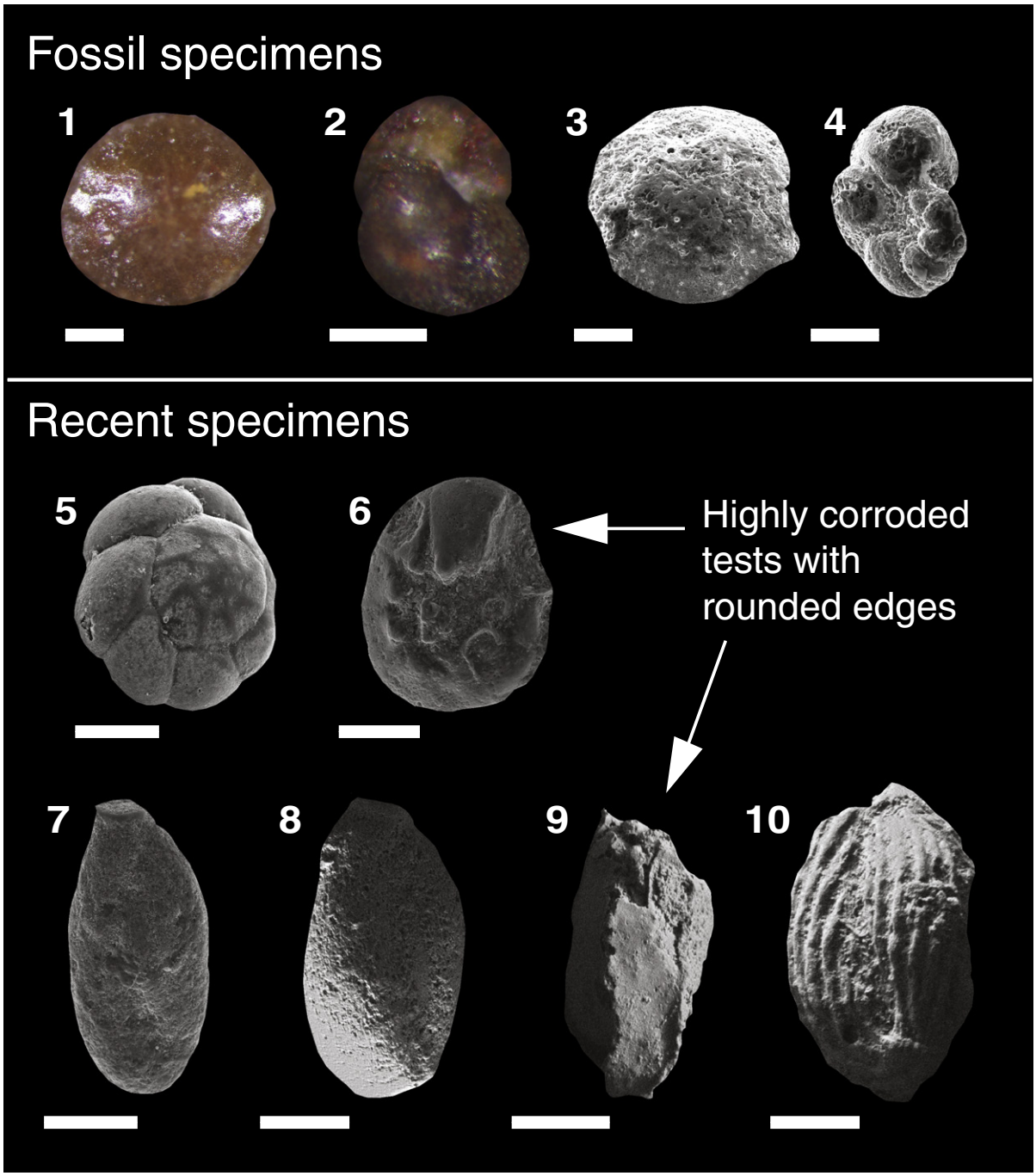

Plate 1. All scale bars are equal to 100 μm. (1–2) Light microscope images of sediment in-filled fossil specimens. (3–4) SEM images of fossil specimens indicating highly corroded and abraded tests. (5) Recent *A. parkinsoniana* ventral view. (6) Recent *A. parkinsoniana* dorsal view. (7–10) Taphonomically altered (corroded, abraded, edge rounded) recent miliolids.

sand was generally the dominant (e.g. D_{90}) particle size throughout the entire deposit and only ranged from 0 to 2Φ; however, the fine component (e.g. D_{10}) of the deposit varied considerably with D_{10} values varying by 6.2Φ (Fig. 3e, f, j; Appendix 1). The deposit thickness also thinned from 25 cm at a distance of 1 km from the shoreline to <5 mm 4.5 km inland (Fig. 4).

The tsunami deposit contained a combination of recent (e.g. calcareous, late Holocene) and fossil (sediment in-filled, calcified, Miocene to Pleistocene) foraminifera. Recent foraminifera were taphonomically altered showing signs of significant fragmentation, edge rounding (abrasion) and dissolution. Fractured edges also showed evidence of edge rounding indicating fragmentation occurred before tsunami deposition. Taphonomic alteration prevented proper species identification except *A. parkinsoniana*, which was present in most samples, although in very low abundances (<20 individuals per 1 cm^3; Plate 1). Miliolids were also found in low abundances. Analyses of the trench sections versus distance inland showed analogous relations to the surface samples regarding the abundances of fossil and recent foraminifera. Recent individuals, although low in abundance, peaked at trenches 5 (~25 individuals per cm^3) and 12 (~29 individuals per cm^3) and decreased by ~50% by trench 48 (~12 individuals per cm^3). At the landward extent of our sediment transect (~4.5 km, trench 86) no recent foraminifera were found (Fig. 3c).

Fossil foraminifera were more robust, calcified, darker in color, highly abraded and more abundant than recent specimens within the tsunami deposit in all trenches (Fig. 5). Abundances of fossil foraminifera within the tsunami deposit peak at trenches 9 and 12 (~102 individuals per cm^3, ~104 individuals per cm^3 respectively) immediately inland of the coastal forest (0.4–0.5 km inland), decrease to less than 3 individuals per cm^3 by trench 86 (Fig. 3b) and contain relatively high abundances of *Amphistegina* spp. (e.g. individual 1 in Plate 1), *Quinqueloculina* spp., and unrecognizable miliolids (Appendices 2, 3). Similarly, large fossil individuals (>250 μm) dominate the area between trench 12 (67%; 22% *Amphistegina* spp.; 43% miliolids) and trench 31 (64%; 13% *Amphistegina* spp.; 40% miliolids), rapidly decrease in abundance at trench 48 (24%; 12% *Amphistegina* spp.; 28% miliolids) and are non-existent by trench 86 (Fig. 3d).

4.3. Vertical changes within the Tōhoku-oki tsunami deposit

The six trench sections (5, 12, 31, 36, 48, 86) are characterized by three distinct units (Figs. 4 and 5). Trenches had basal rice field soil (except at trench 5 where there was a basal forest soil) with a pronounced yellow-brown color, consisting of poorly sorted to very poorly sorted medium sand. This was sharply overlain with a medium-grained sand deposit that transitioned into a muddy-sand unit consisting of clay to fine sand sized particles. The fine component of the muddy-sand layer increased with distance inland and ultimately became the dominant sedimentary unit ranging from very fine sand ($D_{10}=3.8\Phi$) 1.6 km inland to clay ($D_{10}=8.1\Phi$) at ~4 km. The muddy-sand layer was evident at sites greater than 1.2 km from the coastline, but was often discontinuous. The sand and muddy-sand units (where present) together comprise the tsunami deposit. The tsunami deposit generally fined upward and became less sorted, and in some cases (e.g. trench 31) contained finer dark laminae (Fig. 5). Particle sphericity did not show any consistent vertical trends within the tsunami sands or between the tsunami sands and the muddy-sand.

Foraminifera (fossil and recent) are absent within the soil, except at trenches 5 and 31 where very low abundances (11 recent and 65 fossil individuals per cm^3 at trench 5; 3 recent and 53 fossil individuals per cm^3 at trench 31) are found near the contact with the overlying sand suggesting some bioturbation (Fig. 5). Foraminifera are present in the tsunami sand (19 recent and 82 fossil individuals per cm^3) and muddy-sand (8 recent and 10 fossil individuals per cm^3), with little or no variations in abundance with depth, except at trenches containing a muddy sand-layer where abundances of fossil specimens are significantly higher in the sand than in the overlying muddy-sand. However, the proportion of large recent and fossil foraminifera was highest at the bottom of the tsunami deposit and showed a slight upward fining sequence in most trenches. For

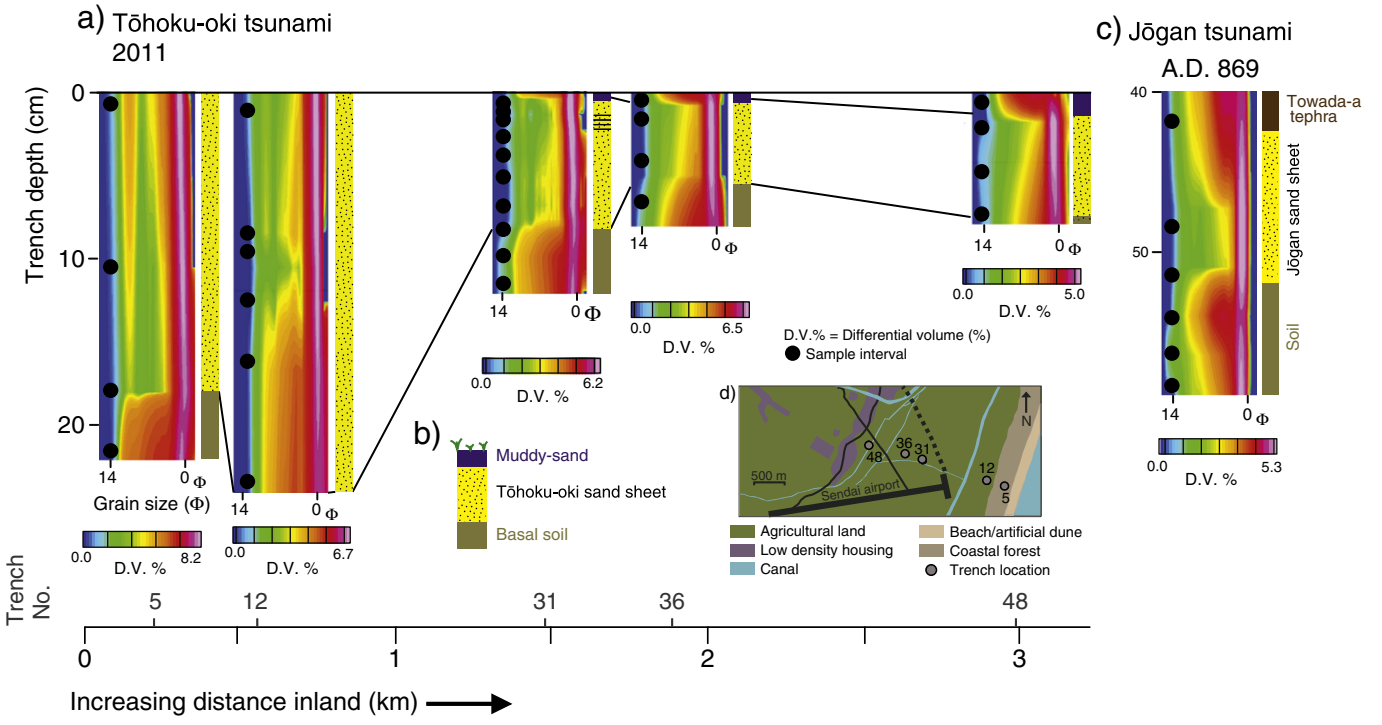

Fig. 4. (a) Particle size distribution (PSD) plots for Tōhoku-oki trench sections along the transect. Facies designations are based on field observations and black dots represent sampling intervals. (b) Generalized stratigraphic section of the Tōhoku-oki tsunami deposit from 1.5 to 2.8 km inland. (c) PSD plot for the Jōgan trench section including the overlying soil and Towada-a tephra deposited by volcanic activity to the north of Sendai in A.D. 870–934 (Fig. 1a). (d) Location of trench sites. For elevation (meters above TP) and distance from the coastline see Fig. 3a.

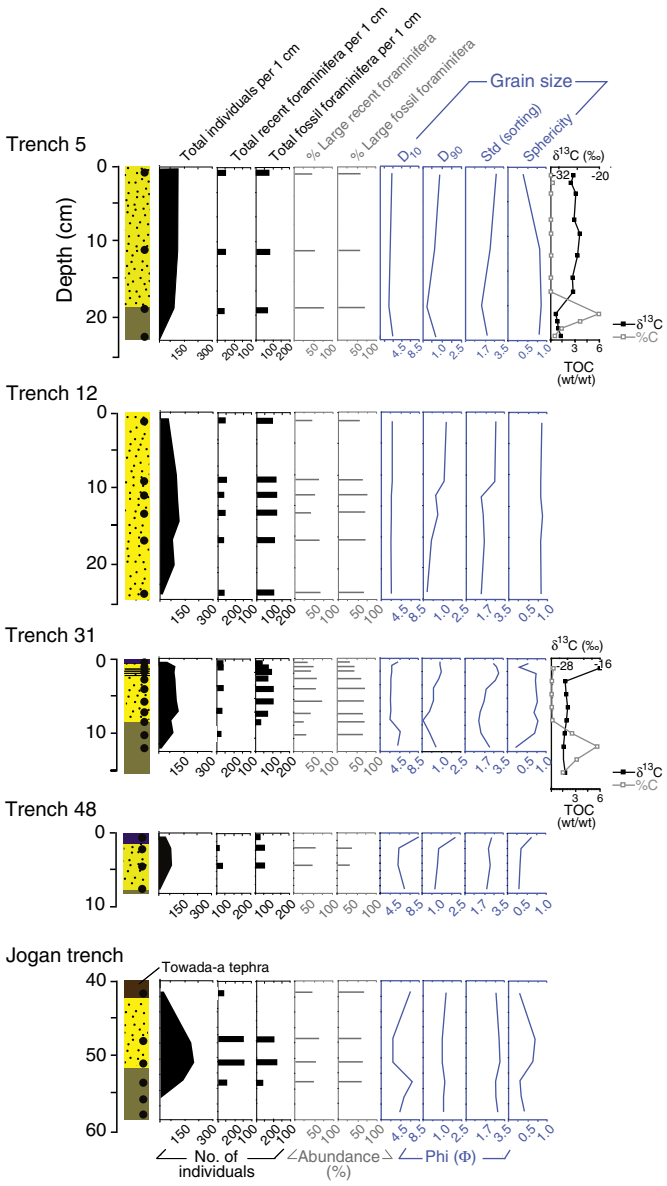

Fig. 5. Grain size and foraminiferal taphonomic data for trenches 5, 12, 31, 48 and Jōgan. $\delta^{13}C$, TOC data for trenches 5 and 31 are shown. Black dots indicate sampling intervals.

example, recent and fossil foraminifera at the base of the tsunami deposit at trench 12 were 63% and 71% large (>250 μm) respectively and decreased to 45% and 56% at the top of the unit. Test size grading was most pronounced in trenches containing capping muddy-sand layers (e.g. trench 31: 70% large sized fossils at the bottom of the tsunami unit, 50% at the top of the sand and 30% in the muddy-sand layer; 70% large sized recent foraminifera at the bottom, 49% at the top of the tsunami sand and 40% in the muddy-sand).

Total organic carbon and $\delta^{13}C$ of two trench sections (5, 31) distinguished between the tsunami deposit and the underlying soil (Fig. 5). In trench 5, $\delta^{13}C$ ranged from −27.0 to −24.8‰ in the tsunami sand and −29.5 to −30.8‰ in the soil. TOC values were notably low in the tsunami deposit (~0.1%) compared with the underlying soil (0.5%–5.9%). Similar to grain size results, three distinct units are distinguished in the TOC and $\delta^{13}C$ profile of trench 31. From 17.5 to 11.5 cm the soil has $\delta^{13}C$ values of −27.8‰ to −27.1‰ and TOC values ranging from 1.5% to 5.7%. The TOC decreases to 0.1% and the $\delta^{13}C$ values increase to −26.3‰ in the tsunami sand. The tsunami muddy-sand shows slightly elevated TOC values (0.3%) and much higher $\delta^{13}C$ (−15.1‰).

4.4. A.D. 869 Jōgan tsunami deposit

We compared the Tōhoku-oki deposit with an older event of similar magnitude, the A.D. 869 Jōgan tsunami (Fig. 1). The Jōgan trench consisted of five stratigraphic units (basal soil, Jōgan tsunami deposit, soil, Towada-a tephra, and overlying soil; Fig. 4c), of which the basal soil, tsunami deposit and soil were sampled and analyzed. The basal soil is composed of a very poorly sorted (StD = 2.8Φ) sandy soil (D_{10} = 5.2Φ, D_{90} = 1.1Φ). The overlying Jōgan tsunami deposit is a 10-cm-thick very poorly sorted (StD = 3.0Φ), medium sand (D_{90} = 1.0Φ). The tsunami deposit is overlain by soil which is itself overlain by the Towada-a tephra (D_{10} = 6.4Φ; StD = 2.7Φ). The contacts between these four units were gradational. The Jōgan tsunami deposit showed similar sedimentological characteristics as the Tōhoku-oki: slight fining in grain size, better sorting, and greater particle sphericity (Fig. 4) from the bottom of the deposit to the top. The Jōgan tsunami deposit showed a pronounced influx of highly spherical sediment (sphericity = 0.7) compared to the overlying Towada-a (0.3) and underlying soil (0.3; Figs. 3h and 5). In the modern environment, highly spherical sediments seem to be originating from the beach (0.8) and dunes (0.9).

Foraminifera were present (~190 recent and ~162 fossil individuals per cm^3) in the tsunami deposit indicating a probable intertidal origin. Low abundances of foraminifera were found in the upper samples of the basal soil (fossil = 42; recent = 65 individuals per cm^3) and the Towada-a tephra (fossil = 3; recent = 16 individuals per cm^3) suggesting bioturbation. This is similar to basal soils underlying the Tōhoku-oki deposit (trenches 5, 31 and 48), where no recent or fossil foraminifera were found below the bioturbated contact (Fig. 5). The recent foraminiferal assemblage of the Jōgan tsunami deposit consisted of *A. parkinsoniana*, various taphonomically altered miliolids and unaltered planktics. This is in contrast to the Tōhoku-oki deposit where no planktics were found. Compared to the Tōhoku-oki deposit, *A. parkinsoniana* individuals were more altered, showing signs of increased abrasion and dissolution. Large test sizes dominate the tsunami deposit and do not appear to show evidence of grading.

5. Discussion

5.1. Stratigraphy and grain size analyses of the 2011 Tōhoku-oki tsunami

Tsunami deposits of Hokkaido Japan (Sawai, 2002), New Zealand (Goff et al., 2001), Papua New Guinea (Morton et al., 2007), Cascadia (Hawkes et al., 2011) and elsewhere have been described on the basis of their lateral, sheet-like geometry, with the deposit thickness tapering inland (Goff et al., 2001; Morton et al., 2007). At Sendai, the tsunami deposit was variable in thickness, extended over a 4.5 km transect, tapered inland from 25 cm to less than 5 mm and contained fine dark laminae interbedded with sand at some trenches (trench 31), as also reported by Szczuciński et al. (2012–this volume) and Richmond et al. (2012–this volume). The Tōhoku-oki sand deposit is similar in grain size (average D_{10} = 4.0Φ, average D_{90} = 0.7Φ) and degree of sorting (StD = 2.2Φ) to modern intertidal (average D_{10} = 1.9Φ, average D_{90} = 0.5Φ; StD = 2.2Φ), beach (D_{10} = 1.5Φ; D_{90} = 0.0Φ; StD = 1.9Φ) and dune (D_{10} = 3.7Φ; D_{90} = 1.4Φ; StD = 3.6Φ) surface samples (Fig. 3e–g) supporting the suggestion of Goto et al. (2011) and Szczuciński et al. (2012–this volume) who ascribe a nearshore to dune origin for the tsunami sand.

The finer underlying rice field soil (average D_{10} = 4.6Φ; average D_{90} = 0.5Φ) sharply transitioned to a coarser sand deposit (average D_{10} = 4.0Φ; average D_{90} = 0.7Φ) that, in some cases, fined upward to a muddy-sand layer (average D_{10} = 7.2Φ; average D_{90} = 1.3Φ). PSD data augmented statistical grain size values by indicating a distinct fine tail at the top of trenches 31, 36 and 48 (Fig. 4). The fining

upward sequence within the Tōhoku-oki deposit is in agreement with several other studies (e.g. Hawkes et al., 2007; Morton et al., 2007; Goodman-Tchernov et al., 2009) and represents entrainment of sediment followed by rapid deposition. The muddy-sand layer that caps the sand deposit at several trenches located at least 1.2 km from the shoreline up to 2.8 km and then becomes dominant represents further waning energy and is likely derived from antecedent rice field soil, canal mud or deeper offshore mud. It is possible that the tsunami scoured deeper offshore (below storm wave base) entraining finer grain sizes that were deposited in areas of sustained flooding. This interpretation is further supported by TOC, $\delta^{13}C$ and foraminiferal results (see below) which suggest an intertidal to beach origin for the muddy-sand layer. Detailed sedimentary descriptions of the deposit are reported by Szczuciński et al. (2012–this volume) and Richmond et al. (2012–this volume).

5.2. Recent and fossil foraminifera as a tsunami indicator

The presence of abundant foraminifera is a characteristic of tsunami deposits (e.g. Hawkes et al., 2007; Kortekaas and Dawson, 2007; Mamo et al., 2009; Pilarczyk and Reinhardt, 2012a, 2012b), but at Sendai their abundance within the sand deposit was low. Hawkes et al. (2007) found up to 1400 individuals per cm^3 in the 2004 Indian Ocean tsunami deposit in Malaysia and Thailand, whereas we only found up to 48 recent individuals per cm^3. The lack of recent foraminifera within intertidal sediments is also anomalous when compared to Matoba (1976) who documented diverse foraminifera in the deeper areas of Sendai Bay (depths of 19–1988 m) and other studies from other Japanese coastlines (e.g. Toba, Mie Prefecture, Hokkaido) that report abundant and diverse assemblages (Okahashi et al., 2002; Nanayama and Shigeno, 2004, 2006). Szczuciński et al. (2012–this volume) also report a surprising paucity of nannoliths (biogenic carbonate) and marine diatoms in intertidal areas as well as in the Tōhoku-oki tsunami deposit. Furthermore, the foraminifera within the tsunami deposit were highly taphonomically altered. Taxonomic identification was impossible except for *A. parkinsoniana*. *A. parkinsoniana* has previously been documented as inhabiting brackish littoral (5–10 m deep) to sub-littoral (<300 m deep) areas in Hokkaido, Sanriku and Boso Peninsula, Japan (Takata et al., 2006; Uchida et al., 2010) and elsewhere (e.g. Debenay et al., 1998), but not in Sendai Bay (Matoba, 1976). Low abundances of *A. parkinsoniana* are found unaltered in post-tsunami intertidal sediment and possible sources include the brackish zone at the confluence of the canals and the sea, or allochthonous sediment that may have been brought in during or post canal construction.

The taphonomic character of recent foraminifera have been used to document overwash deposits because it can provide additional information concerning energy regimes and transport history (e.g. Hawkes et al., 2007; Kortekaas and Dawson., 2007; Satyanarayana et al., 2007; Uchida et al., 2010; Pilarczyk et al., 2011; Pilarczyk and Reinhardt, 2012b). Within the Tōhoku-oki tsunami deposit, recent foraminifera showed evidence of subaerial exposure through a high degree of abrasion (edge rounding), corrosion and fragmentation (Berkeley et al., 2009; Pilarczyk et al., 2011). Contrary to other taphonomic studies of tsunami sediments (e.g. Kortekaas and Dawson, 2007), fragmentation at Sendai was not a function of the tsunami. Rather, edge rounding of fractured surfaces indicates repeated subaerial exposure and significant residence time in the coastal zone (beach and artificial dune). Abundances of recent foraminifera peak in modern dune samples and probably do not represent modern conditions at Sendai since the artificial dune sediment was transported from an unknown source.

Fossil individuals are found in all trenches, including the landward limit of the transect (4.5 km), and show a marked decrease in concentration and size with increasing distance inland. Fossil specimens proved to be marine indicators because they were found predominantly in surface intertidal sediments. Miocene to Pleistocene marine sediments (unconsolidated) and sedimentary rock surrounding the Sendai plain are the probable source of the fossil foraminifera (Fig. 1b). The calcified tests of fossil individuals indicate diagenesis and favor a lithified rock origin over unconsolidated sedimentary units, of which there are two main sources: Jurassic sedimentary rock outcropping on the Oshika Peninsula and near Sōma; and Early Cretaceous marine sedimentary rock off Oshika. Because of the dominating northward longshore drift in Sendai Bay (Hattori, 1967), most fossil foraminifera are more likely to have originated from the south (area near Sōma).

Both fossil and recent foraminifera abundances declined with increasing distance inland. The abundance of large sized individuals (e.g. >250 μm) ranged from 60% to 70% between the coastline and 1.5 km inland where they began to markedly decrease to 30%–35% at 2.5 km inland and finally to a negligible amount (e.g. <1%) at 4.5 km inland. The abrupt decrease in abundance of large sized individuals at 1.2 km inland coincides with the beginning of the muddy-sand (e.g. trench 31 at 1.6 km and trench 48 at 2.4 km) and likely represents waning energy and sustained pooling of marine water.

5.3. TOC and $\delta^{13}C$ trends

Stable carbon isotopes ($\delta^{13}C$) and total organic carbon (TOC) have been used extensively to infer the provenance of organic matter hosted in terrestrial, coastal wetland and marine sediments (e.g. Tyson, 1995; Lamb et al., 2007; Kemp et al., 2010; Vane et al., 2010). Although $\delta^{13}C$ and TOC have the potential to distinguish tsunami sediment from underlying soils primarily because imported marine sands should have low TOC content and higher $\delta^{13}C$ values than the local terrestrial soils, they have seldom been applied.

In trench 5, the basal forest soil has low $\delta^{13}C$ values (−30.8‰) and TOC of up to 6%. Pine roots that are found in the soil have similar $\delta^{13}C$ (−30.4‰), which are consistent with values reported from other forest soils (e.g. Goni and Eglinton, 1996; Goni and Thomas, 2000; Vane et al., 2003) and from the same area by Chagué-Goff et al. (2012–this issue). This suggests a woody terrestrial plant material source for the forest soil. In contrast the overlying tsunami sand has $\delta^{13}C$ values ranging from −27.0‰ to −24.8‰ and very low TOC of about 0.1% (Fig. 5). The $\delta^{13}C$ of marine and open coastal sediments typically range between −18‰ to −23‰ and estuarine sediments range from −26‰ to −23‰ (Hedges and Mann, 1979; Mishima et al., 1999; Wilson et al., 2005). Furthermore, surface sediments from the marine influenced section of Osaka Bay, Japan are characterized by $\delta^{13}C$ of −20‰ to −21‰ (Mishima et al., 1999). In two trench sections containing the Tōhoku-oki deposit we found the $\delta^{13}C$ values of the sand unit to be slightly more depleted in ^{13}C (negative) than that expected for sediment hosting purely marine-derived organic matter, but remain 4.0‰ higher than the underlying soil. A similar contrast in TOC values between the underlying soil and overlying tsunami deposit was more pronounced at trench 31 than trench 5. However the greatest $\delta^{13}C$ change is associated with the transition to the capping muddy-sand layer ($\delta^{13}C = 26.3‰$ to −15.1‰). The minor change in $\delta^{13}C$ between the basal soil and tsunami deposit at trench 31 probably reflects its greater distance inland and thus a larger contribution of terrestrial organic matter sources. The positive values of the muddy-sand may result from sediment containing organic matter from plants utilising the C_4 photosynthetic pathway (range −17 ‰ to −9‰; Deines, 1980). Alternatively, the organic matter is sourced from either marine algae (−16 ‰to −24‰), marine plankton (−13 to −31‰), marine particulate organic carbon (−18‰ to −24‰), marine bacteria (−12‰ to −26‰), sea grasses (marine C_4 plant; −14‰ to −19‰), or possibly cyanobacteria (Deines, 1980; Tyson, 1995). The muddy-sand unit shows evidence of organic matter of marine origin because C_4 plants do not occur in isolation from C_3 plants and would produce a mixed $\delta^{13}C$ signature of about −21‰. The low TOC content of 0.3%

suggests against input from plant organic matter which typically increases overall a coastal sediments TOC content above 0.5%. The contribution of C_4 agricultural plants (maize, sugar cane millet sorghum) which also give overlapping $\delta^{13}C$ can be largely discounted since these crops also tend to yield sediments with high $\delta^{13}C$ and TOC values (1%–5% TOC) due to their cellulose and lignin rich structures.

5.4. Comparison between the Tōhoku-oki and Jōgan tsunami deposits

Historical records mention several tsunamis that have impacted northeast Japan (Minoura and Nakaya, 1991; Minoura et al., 2001). However, the A.D. 869 Jōgan tsunami is reported to be similar to the Tōhoku-oki event in terms of the extent of inundation (Goto et al., 2011). Both tsunamis deposited a laterally extensive, landward thinning sand deposit that extended to distances greater than 2 km from the coast (Goto et al., 2011; Sugawara et al., 2011b).

Grain size distributions were effective in discriminating the sand units (medium sand) deposited by both the Tōhoku-oki and Jōgan tsunamis from the finer soils. At the studied trench, the Jōgan sand deposit could be distinguished from the underlying basal soil and overlying Towada-a tephra even though contacts were gradational. Both tsunami deposits consisted of very poorly sorted (Tōhoku-oki: 2.0Φ; Jōgan: 3.0Φ) medium sand (Tōhoku-oki: $D_{90} = 0.7\Phi$; Jōgan: $D_{90} = 1.0\Phi$) that fined upward (Fig. 4). Notable differences between the deposits include the absence of a muddy-sand layer and laminae in the Jōgan deposit. This may be evidence of depositional style (e.g. magnitude of earthquake, sediments available for transport, flow depth, etc.), or post-depositional change whereby bioturbation obscures internal structures (Szczuciński, 2012). The absence of a muddy-sand layer could also be related to the location of the Jōgan trench, that was sampled 1.5 km from the present coastline, which is equivalent to ~0.5 km from the paleo-coastline. No muddy-sand units were reported from the Tōhoku-oki tsunami within 1.2–1.5 km from the shoreline.

The recent and fossil foraminifera also showed broad similarities and noticeable differences. Foraminifera were more abundant within the Tōhoku-oki and Jōgan tsunami deposits although bioturbation may have resulted in their occurrence in the underlying soil, and in the case of Jōgan, also the overlying units. In the Jōgan tsunami deposit concentrations of fossil and recent individuals were similar (recent = 190 individuals per cm^3; fossil = 162 individuals per cm^3), which is in contrast to the Tōhoku-oki deposit where fossil foraminifera are more abundant. The recent assemblage of foraminifera in the Jōgan sequence was dominated by *A. parkinsoniana* and miliolids, but there was a noticeable presence of planktic individuals. Planktic foraminifera have also been used to document tsunami sediments from the Indian Ocean (Hawkes et al., 2007), the Aegean Sea (Minoura et al., 2012) and the Arabian Sea (Pilarczyk and Reinhardt, 2012b).

6. Conclusions

The 2011 Tōhoku-oki tsunami shows marked trends of inland fining and thinning and can be discriminated from the underlying soil by an abrupt increase in grain size (medium sand) and the notable appearance of recent and fossil foraminifera. TOC and $\delta^{13}C$ analysis of the Tōhoku-oki deposit also revealed a contrast between the soil and the overlying tsunami unit at one trench and corroborates grain size and foraminiferal results that indicate an intertidal source for the sand. Problems of identification of recent foraminifera along the Sendai transect limit their utility; however, the added use of taphonomy (test condition, fossil specimens) helped to constrain sediment provenance and hydrodynamic regime.

Supplementary data to this article can be found online at http://dx.doi.org/10.1016/j.sedgeo.2012.08.011.

Acknowledgements

Members of the UNESCO-IOC (Intergovernmental Oceanographic Commission) team to Japan provided samples and guidance. Among them we especially thank Kazuhisa Goto and Bruce Jaffe for their involvement in executing this field survey. We also thank Daisuke Sugawara, Yuichi Nishimura and Shigehiro Fujino for their assistance while on site in Japan, Kazuhisa Goto for providing survey data and Doug Jerolmack for the use of his camsizer. C. Vane publishes with the permission of the Executive Director, British Geological Survey (NERC). The work was supported in part by UNESCO-IOC, The U.S. Geological Survey and a National Science Foundation award (EAR-0842728). This paper is a contribution to IGCP 588.

References

Association of Japanese Geographers, 2011. Map of tsunami inundation reported by Tsunami Damage Team. http://danso.env.nagoya-u.ac.jp/20110311/map/574017Sendaikukou.jpg.

Berkeley, A., Perry, C.T., Smithers, S.G., 2009. Taphonomic signatures and patterns of test degradation on tropical, intertidal benthic foraminifera. Marine Micropaleontology 73, 148–163.

Bernard, E.N., Robinson, A.R., 2009. Tsunamis. The Sea, vol. 15. Harvard University Press, Cambridge, MA. 450 pp.

Blott, S.J., Pye, K., 2001. Gradistat: a grain size distribution and statistics package for the analysis of unconsolidated sediments. Earth Surface Processes and Landforms 26, 1237–1248.

Bondevik, S., Lovholt, F., Harbitz, C., Mangerud, J., Dawson, A., Svendsen, J.I., 2005. The Storegga Slide tsunami—comparing field observations with numerical observations. Marine and Petroleum Geology 22, 195–208.

Chagué-Goff, C., 2010. Chemical signatures of palaeotsunamis: a forgotten proxy? Marine Geology 271, 67–71.

Chagué-Goff, C., Dawson, S., Goff, J., Zachariasen, J., Berryman, K., Garnett, D., Waldron, H., Mildenhall, D., 2002. A tsunami (ca. 6300 years BP) and other Holocene environmental changes, northern Hawke's Bay, New Zealand. Sedimentary Geology 150, 89–102.

Chagué-Goff, C., Schneider, J., Goff, J.R., Dominey-Howes, D., Strotz, L., 2011. Expanding the proxy toolkit to help identify past events—lessons from the 2004 Indian Ocean tsunami and the 2009 South Pacific tsunami. Earth-Science Reviews 107, 107–122.

Chagué-Goff, C., Andrew, A., Szczuciński, W., Goff, J., Nishimura, Y., 2012. Geochemical signatures up to the maximum inundation of the 2011 Tohoku-oki tsunami—implications for the 869 AD Jogan and other palaeotsunamis. Sedimentary Geology 282, 65–77 (this issue).

Chagué-Goff, C., Niedzielski, P., Wong, H.K.Y., Szczuciński, W., Sugawara, D., Goff, J., 2012. Environmental impact assessment of the 2011 Tohoku-oki tsunami on the Sendai plain. Sedimentary Geology 282, 175–187 (this issue).

Cisternas, M., Atwater, B.F., Torrejon, F., Sawai, Y., Machuca, G., Lagos, M., Eipert, A., Youlton, C., Salgado, I., Kamataki, T., Shishikura, M., Rajendran, C.P., Malik, J.K., Rizal, Y., Husni, M., 2005. Predecessors of the giant 1960 Chile earthquake. Nature 437, 404–407.

Debenay, J., Beneteau, E., Zhang, J., Stouff, V., Geslin, E., Redois, F., Fernandez-Gonzalez, M., 1998. *Ammonia beccarii* and *Ammonia tepida* (Foraminifera): morphofunctional arguments for their distinction. Marine Micropaleontology 34, 235–244.

Deines, P., 1980. The isotopic composition of reduced organic carbon. In: Fritz, P., Fontes, J.C. (Eds.), Handbook of Environmental Isotope Geochemistry. Elsevier, Amsterdam, pp. 329–426.

Donato, S.V., Reinhardt, E.G., Boyce, J.I., Pilarczyk, J.E., Jupp, B.P., 2009. Particle-size distribution of inferred tsunami deposits in Sur Lagoon, Sultanate of Oman. Marine Geology 257, 54–64.

Geological Survey of Japan, AIST (ed.), 2009. Seamless digital geological map of Japan 1:200,000. December 15, 2009 version. Research Information Database DB084, Geological Survey of Japan, National Institute of Advanced Industrial Science and Technology.

Goff, J., Chagué-Goff, C., 1999. A late Holocene record of environmental changes from coastal wetlands: Abel Tasman National Park, New Zealand. Quaternary International 56, 39–51.

Goff, J., Chagué-Goff, C., Nichol, S., 2001. Palaeotsunami deposits: a New Zealand perspective. Sedimentary Geology 143, 1–6.

Goff, J., Chagué-Goff, C., Dominey-Howes, D., McAdoo, B., Cronin, S., Bonté-Grapetin, M., Nichol, S., Horrocks, M., Cisternas, M., Lamarche, G., Pelletier, B., Jaffe, B., Dudley, W., 2011. Palaeotsunamis in the Pacific. Earth-Science Reviews 107, 141–146.

Goni, M.A., Eglinton, T.I., 1996. Stable carbon isotopic analyses of lignin-derived CuO oxidation products by isotope ratio monitoring gas chromatography mass spectrometry (irm–GC–MS). Organic Geochemistry 24 (6–7), 601–615.

Goni, M.A., Thomas, K.A., 2000. Sources and transformations of organic matter in surface soils and sediments from a tidal estuary (north inlet, South Carolina, USA). Estuaries 23 (4), 548–564.

Goodman-Tchernov, B.N., Dey, H.W., Reinhardt, E.G., McCoy, F., Mart, Y., 2009. Tsunami waves generated by the Santorini eruption reached eastern Mediterranean shores. Geology 37, 943–946.

Goto, K., Chagué-Goff, C., Fujino, S., Goff, J., Jaffe, B., Nishimura, Y., Richmond, B., Sugawara, D., Szczucinski, W., Tappin, D.R., Witter, R.C., Yulianto, E., 2011. New insights of tsunami hazard from the 2011 Tōhoku-oki event. Marine Geology 290, 46–50.
Hattori, M., 1967. Recent sediments of Sendai Bay, Miyagi Prefecture, Japan. Scientific Reports of Tohoku University, 2nd Series (Geology), 39, pp. 1–61.
Hawkes, A.D., Bird, M., Cowie, S., Grundy-Warr, C., Horton, B.P., Tan Shau Hwai, A., Law, L., Macgregor, C., Nott, J., Eong Ong, J., Rigg, J., Robinson, R., Tan-Mullins, M., Tiong, T., Yasin, Z., Wan Aik, L., 2007. Sediments deposited by the 2004 Indian Ocean tsunami along the Malaysia–Thailand Peninsula. Marine Geology 242, 169–190.
Hawkes, A.D., Horton, B.P., Nelson, A.R., Vane, C.H., Sawai, Y., 2011. Coastal subsidence in Oregon, USA, during the giant Cascadia earthquake of AD 1700. Quaternary Science Reviews 30, 364–376.
Hayward, B.W., Holzmann, M., Grenfell, H.R., Pawlowski, J., Triggs, C.M., 2004. Morphological distinction of molecular types in Ammonia—towards a taxonomic revision of the world's most commonly misidentified foraminifera. Marine Micropaleontology 50, 237–271.
Hedges, J.I., Mann, D.C., 1979. The lignin geochemistry of marine sediments from the southern Washington coast. Geochimica et Cosmochimica Acta 43, 1809–1818.
Hemphill-Haley, E., 1995. Diatom evidence for earthquake-induced subsidence and tsunami 300 years ago in southern coastal Washington. Geological Society of America Bulletin 107 (3), 367–378.
Horton, B.P., Edwards, R.J., 2006. Quantifying Holocene sea level change using intertidal foraminifera: lessons from the British Isles. Cushman Foundation for Foraminiferal Research, Special Publication, 40. 97 pp.
Ito, Y., Tsuji, T., Osada, Y., Kido, M., Inazu, D., Hayashi, Y., Tsushima, H., Hino, R., Fujimoto, H., 2011. Frontal wedge deformation near the source region of the 2011 Tohoku-oki earthquake. Geophysical Research Letters 38 http://dx.doi.org/10.1029/2011GL048355.
Jankaew, K., Atwater, B.F., Sawai, Y., Choowong, M., Charoentitirat, T., Martin, M.E., Prendergast, A., 2008. Medieval forewarning of the 2004 Indian Ocean tsunami in Thailand. Nature 455, 1228–1231.
Kelsey, H.M., Nelson, A.R., Hemphill-Haley, E., Witter, R.C., 2005. Tsunami history of an Oregon coastal lake reveals a 4600 yr record of great earthquakes on the Cascadia subduction zone. GSA Bulletin 117 (7–8), 1009–1032.
Kemp, A.C., Vane, C.H., Horton, B.P., Culver, S.J., 2010. Stable carbon isotopes as potential sea-level indicators in salt marshes, North Carolina, USA. The Holocene 20 (4), 623–636.
Koper, K.D., Hutko, A.R., Lay, T., Ammon, C.J., Kanamori, H., 2011. Frequency-dependent rupture process of the 2011 Mw 9.0 Tohoku-oki Earthquake: comparison of short-period P wave backprojection images and broadband seismic rupture models. Earth Planets Space 63, 599–602.
Kortekaas, S., Dawson, A.G., 2007. Distinguishing tsunami and storm deposits: an example from Martinhal, SW Portugal. Sedimentary Geology 200, 208–221.
Lamb, A.L., Vane, C.H., Wilson, G.P., Rees, J.G., Moss-Hayes, V.L., 2007. Assessing $\delta^{13}C$ and C/N ratios from organic material in archived cores as Holocene sea level and palaeoenvironmental indicators in the Humber Estuary, UK. Marine Geology 244, 109–128.
Loeblich, A.R., Tappan, H., 1987. Foraminiferal Genera and Their Classification. Van Nostrand Rienhold Co., New York.
Machida, H., Arai, F., 2003. Atlas of Tephra in and Around Japan, revised edition. University of Tokyo Press, Tokyo . 336 pp.
Mamo, B., Strotz, L., Dominey-Howes, D., 2009. Tsunami sediments and their foraminiferal assemblages. Earth-Science Reviews 96, 263–278.
Matoba, Y., 1976. Recent foraminiferal assemblages off Sendai, northeast Japan. In: Schafer, C.T., Pelletier, B.R. (Eds.), First International Symposium on Benthic Foraminifera of Continental Margins, Part A Ecology and Biology: Maritime Sediments, Special Publication, No. 1, pp. 205–220.
Minoura, K., Nakaya, S., 1991. Traces of tsunami preserved in inter-tidal lacustrine and marsh deposits: some examples from northeast Japan. Journal of Geology 99, 265–287.
Minoura, K., Nakaya, S., Uchida, M., 1994. Tsunami deposits in a lacustrine sequence of the Sanriku coast, northeast Japan. Sedimentary Geology 89, 25–31.
Minoura, K., Imamura, F., Sugawara, D., Kono, Y., Iwashita, T., 2001. The 869 Jogan tsunami deposit and recurrence interval of large-scale tsunami on the Pacific coast of northeast Japan. Journal of Natural Disaster Science 23, 83–88.
Minoura, K., Imamura, F., Kuran, U., Nakamura, T., Papadopoulos, G.A., Takahashi, T., Yalciner, A.C., 2012. Discovery of Minoan tsunami deposits. Geology 28 (1), 59–62.
Mishima, Y., Hoshika, A., Tanimoto, T., 1999. Depositional rates of terrestrial and marine organic carbon in the Osaka Bay, Seto Inland Sea, Japan determined using carbon and nitrogen stable isotope ratios in the sediment. Journal of Oceanography 55, 1–11.
Mori, N., Takahashi, T., Yasuda, T., Yanagisawa, H., 2011. Survey of 2011 Tohoku earthquake tsunami inundation and run-up. Geophysical Research Letters 38 http://dx.doi.org/10.1029/2011GL049210.
Morton, R., Gelfenbaum, G., Jaffe, B., 2007. Physical criteria for distinguishing sandy tsunami and storm deposits using modern examples. Sedimentary Geology 200, 184–207.
Nanayama, F., Shigeno, K., 2004. An overview of onshore tsunami deposits in coastal lowland and our sedimentological criteria to recognize them. Memoirs of the Geological Society of Japan 58, 19–33.
Nanayama, F., Shigeno, K., 2006. Inflow and outflow facies from the 1993 tsunami in southwest Hokkaido. Sedimentary Geology 187, 139–158.
Okahashi, H., Akimoto, K., Mitamura, M., Hirose, K., Yasuhara, M., Yoshikawa, S., 2002. Event deposits found in coastal marsh in Osatsu, Toba, central Japan. Chikyu Monthly 24, 698–703.
Ozawa, S., Nishimura, T., Suito, H., Kobayashi, T., Tobita, M., Imakiire, T., 2011. Coseismic and postseismic slip of the 2011 magnitude 9 Tohoku-oki earthquake. Nature 475, 373–376.
Patterson, R.T., Fishbein, E., 1989. Re-examination of the statistical methods used to determine the number of point counts needed for micropaleontological quantitative research. Journal of Paleontology 63 (2), 245–248.
Pilarczyk, J.E., Reinhardt, E.G., 2012a. Homotrema rubrum (Lamarck) taphonomy as an overwash indicator in marine ponds on Anegada, British Virgin Islands. Natural Hazards 63, 85–100.
Pilarczyk, J.E., Reinhardt, E.G., 2012b. Testing foraminiferal taphonomy as a tsunami indicator in a shallow arid system lagoon: Sur, Sultanate of Oman. Marine Geology 295–298, 128–136.
Pilarczyk, J.E., Reinhardt, E.G., Boyce, J.I., Schwarcz, H.P., Donato, S.V., 2011. Assessing surficial foraminiferal distributions as an overwash indicator in Sur Lagoon, Sultanate of Oman. Marine Micropaleontology 80, 62–73.
Pinegina, T.K., Bourgeois, J., Bazanova, L.I., Melekestsev, I.V., Braitseva, O.A., 2003. A millennial-scale record of Holocene tsunamis on the Kronotskiy Bay coast, Kamchatka, Russia. Quaternary Research 59, 36–47.
Richmond, B., Szczuciński, W., Chagué-Goff, C., Goto, K., Sugawara, D., Witter, R., Tappin, D.R., Jaffe, B., Fujino, S., Nishimura, Y., Goff, J., 2012. Erosion, deposition and landscape change on the Sendai coastal plain, Japan resulting from the March 11, 2011 Tohoku-oki tsunami. Sedimentary Geology 282, 27–39 (this volume).
Saito, Y., 1991. In: MacDonald, D.I.M. (Ed.), Sequence stratigraphy on the shelf and upper slope in response to the latest Pleistocene–Holocene sea-level changes off Sendai, northeast Japan, Sedimentation, Tectonics and Eustacy, Sequence Stratigraphy: International Assocaition of Sedimentologists Special Publication, 12, pp. 133–150.
Sambridge, M., Braun, J., McQueen, H., 1995. Geophysical parametrization and interpolation of irregular data using natural neighbors. Geophysical Journal International 122, 837–857.
Satake, K., Namegaya, Y., Yamaki, S., 2008. Numerical simulation of the A. D. 869 Jogan tsunami in Ishinomaki and Sendai Plains. Annual Report of Active Fault and Paleoearthquake Research 8, 71–89.
Sato, M., Ishikawa, T., Ujihara, N., Yoshida, S., Fujita, M., Mochizuki, M., Asada, A., 2011. Displacement above the hypocenter of the 2011 Tohoku-oki earthquake. Science 332, 1395.
Satyanarayana, K., Reddy, A.N., Jaiprakash, B.C., Chidambaram, L., Srivastava, S., Bharktya, D.K., 2007. A note on foraminifera, grain size and clay mineralogy of tsunami sediments from Karaikal–Nagore–Nagapattiuam Beaches, Southeast Coast of India. Journal Geological Society of India 69, 70–74.
Sawai, Y., 2002. Evidence for 17th-century tsunamis generated on the Kuril–Kamchatka subduction zone, Lake Tokotan, Hokkaido, Japan. Journal of Asian Earth Sciences 20, 903–911.
Sawai, Y., Fujii, Y., Fujiwara, O., Kamataki, T., Komatsubara, J., Okamura, Y., Satake, K., Shishikura, M., 2008a. Marine incursions of the past 1500 years and evidence of tsunamis at Suijin-numa, a coastal lake facing the Japan Trench. The Holocene 18, 517–528.
Sawai, Y., Shishikura, M., Komatsubara, J., 2008b. A study of paleotsunami using had corer in Sendai plain (Sendai City, Natori City, Iwanuma City, Watari Town, Yamamoto Town), Miyagi, Japan. Annual Report of Active Fault and Paleoearthquake Researches, 8, pp. 17–70 (in Japanese with English abstract).
Sugawara, D., Imamura, F., 2010. Geological and historical traces of the 869 Jogan tsunami field guide of half-day field trip in Sendai. The 3rd International Tsunami Field Symposium, Sendai, Sanriku and Okinawa, 10–16 April 2010.
Sugawara, D., Goto, K., Chagué-Goff, C., Fujino, S., Goff, J., Jaffe, B., Nishimura, Y., Richmond, B., Szczucinki, W., Tappin, D.R., Witter, R., Yulianto, E., 2011a. Initial field survey report of the 2011 East Japan Tsunami in Sendai, Natori and Iwanuma cities. UNESCO-IOC International Tsuanmi Survey Team . 16 pp.
Sugawara, D., Imamura, F., Matsumoto, H., Goto, K., Minoura, K., 2011b. Reconstruction of the AD 869 Jogan earthquake induced tsunami by using the geological data. Journal of Japanese Society of Natural Disaster Science 29, 501–516.
Sugawara, D., Imamura, F., Goto, K., Matsumoto, H., Minoura, K., 2012. The 2011 Tohoku-oki earthquake tsunami: similarities and differences to the 869 Jogan tsunami on the Sendai plain. Pure and Applied Geophysics http://dx.doi.org/10.1007/s00024-012-0460-1.
Szczuciński, W., 2012. The post-depositional changes of the onshore 2004 tsunami deposits on the Andaman Sea coast of Thailand. Natural Hazards 60, 115–133.
Szczuciński, W., Kokociński, M., Rzeszewski, M., Chagué-Goff, C., Cacho, M., Goto, K., Sugawara, D., 2012. Sediment sources and sedimentation processes of 2011 Tohoku-oki tsunami deposits on the Sendai Plain, Japan — Insights from diatoms, nannoliths and grain size distribution. Sedimentary Geology 282, 40–56 (this volume).
Takata, H., Takayasu, K., Hasegawa, S., 2006. Foraminifera in an organic-rich, brackish-water lagoon, Lake Saroma, Hokkaido, Japan. Journal of Foraminiferal Research 36, 44–60.
Tamura, T., Masuda, F., 2004. Inner shelf to shoreface depositional sequence in the Sendai coastal prism, Pacific coast of northeastern Japan: spatial and temporal growth patterns in relation to Holocene relative sea-level change. Journal of Asian Earth Sciences 23, 567–576.
Tamura, T., Masuda, F., 2005. Bed thickness characteristics of inner-shelf storm deposits associated with a transgressive to regressive Holocene wave-dominated shelf, Sendai coastal plain, Japan. Sedimentology 52, 1375–1395.
Tyson, R.V., 1995. Sedimentary Organic Matter: Organic Facies and Palynofacies. Chapman Hall, London.
Uchida, J., Fujiwara, O., Hasegawa, S., Kamataki, T., 2010. Sources and depositional processes of tsunami deposits: analysis using foraminiferal tests and hydrodynamic verification. Island Arc 19, 427–442.

Vane, C.H., Drage, T.C., Snape, C.E., 2003. Biodegradation of Oak (Quercus alba) wood during growth of the shiitake mushroom (lentinula edodes): a molecular approach. Journal of Agricultural and Food Chemistry 51, 947–956.

Vane, C.H., Kim, A.W., McGowan, S., Leng, M.J., Heaton, T.H.E., Kendrick, C.P., Coombs, P., Yang, H., Swann, G.E.A., 2010. Sedimentary records of sewage pollution using faecal markers in contrasting peri-urban shallow lakes. Science of the Total Environment 409 (2), 345–356.

Wilson, G.P., Lamb, A.L., Leng, M.J., Gonzalez, S., Huddart, D., 2005. $\delta^{13}C$ and C/N as potential coastal palaeoenvironmental indicators in the Meresy Estuary, UK. Quaternary Science Reviews 24, 2015–2029.

Yamada, I., Shoji, S., 1981. The Late Holocene felsic tephra in Miyagi Prefecture. Journal of the Pedological Society of Japan 52, 155–158.